Impact of Building Morphological Indicators on Solar Potential: Validation Analysis of Vertical Obstruction Factor (VOF)

Li Yirong[1], Liu Yu[1], Lei Zhuo[1], Liu Siyi[1], and Song Jie[1]

1 Northwestern Polytechnical University, Xi 'an(China)

Abstract

Integrating solar potential into architectural and urban planning requires an accurate assessment of sunlight obstruction among buildings. This study evaluates the applicability of the Vertical Obstruction Factor (VOF)—an index previously validated only in Lhasa, China—in a different climatic and morphological context: Xi'an. Two key findings are reported: (1) In Xi'an, VOF is significantly correlated with solar potential indicators ($p < 0.05$); (2) The threshold values of solar potential differ markedly between the two cities. In Xi'an, the minimum VOF threshold reaches －0.35, whereas in Lhasa, the maximum VOF threshold is －0.1. Overall, this study confirms the cross-regional applicability of VOF under varying climatic and morphological conditions, providing a quantitative reference for optimizing solar-oriented residential layouts.

Keywords: Vertical Obstruction Factor (VOF), Building morphology, Solar potential, Cross-regional validation, Threshold effect

1.Introduction

1.1. Background

Solar energy is a key resource for achieving urban sustainability, and building morphology plays a crucial role in determining its acquisition efficiency. Significant regional variations in latitude, altitude, and solar radiation levels have led to an increasing demand for location-specific solar planning strategies (Liu et al., 2024). For example, Lhasa (29.66° N; elevation 3,650 m; annual solar radiation $1{,}700 kW \cdot h(m^2 \cdot a)^{-1}$) and Xi'an (34.26° N; elevation 1,027 m; annual solar radiation $1{,}300 kW \cdot h(m^2 \cdot a)^{-1}$; data source: CSWD) exhibit stark contrasts in geographic and climatic conditions. The Vertical Obstruction Factor (VOF), proposed by (Wenqiang et al., 2022), quantifies multidirectional shading effects and offers a more comprehensive metric than traditional sunlight distance indicators. Although the VOF has been validated in Lhasa, its applicability to other urban contexts remains uncertain. This study focuses on Xi'an to examine the relationship between VOF and solar potential, and evaluates the adaptability of the VOF metric across different climatic and morphological conditions through a comparative analysis with Lhasa.

1.2. Literature Review

The impact of building morphology on solar energy potential has become a prominent topic in recent research on energy-efficient architecture. Numerous studies have demonstrated that parameters such as building form, façade orientation, and obstruction factors directly affect the amount of solar radiation received by buildings. A review of studies conducted between 2011 and 2022 on urban morphology indicators (UMIs) and solar radiation acquisition revealed that in sixteen independent investigations, building height (BH), building spacing, building height variation (BHV), and sky view factor (SVF) were positively correlated with solar radiation acquisition (SRA), whereas building density (BD), plot ratio (PR), street canyon aspect ratio (SCAR), verticality (Vert), and building height difference (BHD) exhibited negative correlations with SRA (Liu et al., 2024). Some morphological indicators yielded consistent conclusions across most boundary conditions, suggesting the potential for generalized optimization strategies, while others varied under different conditions, indicating the need for further investigation into their relationships.

Among these factors, the influence of floor area ratio (FAR) on solar energy potential has shown partial

10.18086/swc.2025.08.11 Available at http://proceedings.ises.org

consistency across different studies.Li et al. (2024), in a case study conducted in Nanjing, reported a significant negative correlation between FAR and both photovoltaic power generation (PVa) and solar radiation (SOL). Specifically, as FAR increased from 3 to 7, the unit-area solar radiation (SOLp) declined markedly. Similarly, Zhu et al. (2020), in a study of high-density residential areas in Shanghai, found that although rooftop area remained sufficient as FAR rose from 2 to 10, the proportion of qualified façade area decreased substantially from 40–60% to 10–28%. In Macau, Yang et al. (2024) observed that regression analysis of solar potential indicators SRU_{600} and SRU_{400} produced R^2 values of 0.723 and 0.769, respectively, highlighting the significant role of FAR in shaping solar accessibility. Collectively, these empirical studies and case-based analyses provide strong evidence of a significant negative correlation between FAR and solar energy potential.

Although several studies have demonstrated strong correlations between urban morphology indicators (UMIs) and solar radiation acquisition (SRA), the strength of the fitting results varies considerably across different cases. For instance, Poon et al. (2020) found a strong correlation between the street canyon aspect ratio (SCAR) and SRA, with a coefficient of determination (R^2) of 0.91, indicating that SCAR serves as a reliable indicator of façade-level solar radiation. In contrast, Tian and Xu (2021) also identified correlations between SCAR and both rooftop and façade SRA, but the corresponding R^2 values were only 0.55 and 0.38, respectively.

Similarly, while there is general agreement on the importance of building orientation in influencing SRA, the optimal orientation thresholds differ under varying boundary conditions. For example, a study conducted in Tlemcen, Algeria, revealed that buildings oriented within 45° of due south receive higher levels of solar radiation (Mahaya et al., 2022), whereas research in Cairo, Egypt, suggested that the optimal orientation range lies between 30° and 60° (Ibrahim et al., 2022).

Li (2023) conducted research on residential areas in Lhasa that further underscored the significance of morphological indicators in determining solar potential. The study demonstrated that when the winter solar shape coefficient (FW) is not lower than 0.08, overall solar acquisition indicators remain relatively high. Moreover, as the Vertical Obstruction Factor (VOF) increases, the solar potential also improves; in particular, when VOF exceeds zero, the overall solar performance of buildings is significantly enhanced(Li, 2023).

However, existing research has yet to systematically validate the applicability of VOF and FW in residential areas of Xi'an. Given the substantial differences in climate, geography, and urban morphology between Xi'an and Lhasa, it remains uncertain whether similar conclusions can be drawn for both regions. As a representative mid-latitude city, Xi'an exhibits distinctive morphological characteristics that may influence solar potential. Therefore, the present study aims to evaluate the feasibility of applying FW to residential buildings in Xi'an and to compare its applicability across both regions.

2.Methodology

2.1. Simulation

This study consists of two main components: (1) Validation of the correlation between the Vertical Obstruction Factor (VOF) and solar energy potential based on 50 residential sites in Xi'an; (2) Threshold analysis of VOF under varying D/H ratios using typical obstruction models, with comparative evaluation against data from Lhasa.Samples were selected using a stratified random sampling method, covering both urban core and suburban areas. Three-dimensional models were constructed in Rhino, with detailed annotations of building height, spacing, and orientation. Layouts were further optimized using a genetic algorithm to ensure realistic and efficient site configurations. Obstruction analysis focused on typical linear residential layouts to ensure the accuracy of VOF calculations.

Using the Ladybug plugin and climate data for Xi'an from the China Standard Weather Data (CSWD), annual and heating-season (November 15 to March 15) solar radiation on building surfaces was simulated. Four key solar potential indicators were extracted: Annual Solar Radiation per Unit Area (ASU), Heating Season Solar Radiation per Unit Area (HSU), Share of Surface Area above 800 $kW \cdot h(m^2 \cdot a)^{-1}$ (SA_{800}), and Share of Solar Radiation above 800 $kW \cdot h(m^2 \cdot a)^{-1}$ (SS_{800}). Pearson correlation analysis ($p < 0.01$) was employed to evaluate the relationship between VOF and these indicators.In the threshold analysis, a series of typical models with varying D/H ratios were generated by adjusting the height of the obstructing buildings, and the corresponding VOF values were calculated for both regions using the same set of models. Corresponding VOF values were calculated, and their relationships with solar potential indicators were plotted to identify regional response differences and critical thresholds between Xi'an and Lhasa.

2.2. Calculation Formula

（1）Building Morphology Indicator—Vertical Obstruction Factor (VOF)

$$VOF = \sum \overline{F_i} \times X_i \quad \text{(eq. 1)}$$

Calculation steps:

- Divide solar azimuth sectors from sunrise to sunset on the winter solstice, with angles denoted as α .（Fig. 1）
- Define measurement point A on the obstructed building, partition surrounding areas into shaded/unshaded zones, and draw angle bisectors within each zone.（Fig. 2）
- Calculate for each radial segment: T_i (Tangent of solar altitude angle),$S_i = H/D$: Ratio of obstruction height to spacing.
- Determine shading status:If $C_i = T_i - S_i > 0$: Unshaded ;If $C_i < 0$: Shaded .
- Apply solar direct irradiance weighting:$IR = I_j/I_{MAX}$, Compute weighted $F_i = IR \times C_i$,then average $\overline{F_i}$ per zone.
- Where $(X_i = \beta_i/\alpha)$ proportion of sector central angle.Calculate the sum of each region $\overline{F_i}$ by weighting.

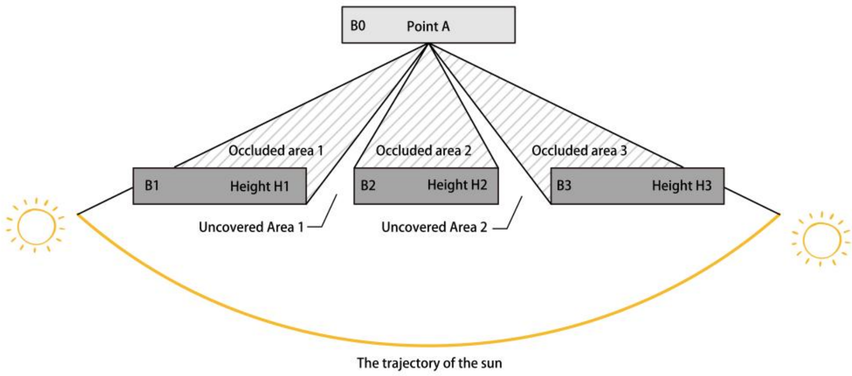

Figure. 1: Delineating sheltered and sheltered areas

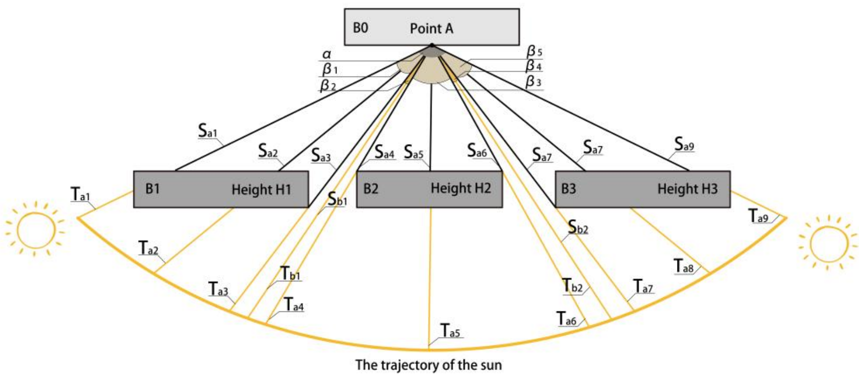

Figure. 2: Calculated line segments and angles for VOF (boundary lines, angle bisectors)

（2）Solar Energy Potential Indicators

1)Annual Solar Radiation per Unit Surface Area (ASU)

Definition: The ratio of the total annual solar radiation received by the building envelope to its surface area ($kW \cdot h(m^2 \cdot a)^{-1}$), reflecting the overall potential for solar energy utilization.

$$\mathrm{ASU} = \frac{\sum \text{ Annual Solar Radiation}}{\sum \text{ Building Surface Area}} \quad \text{(eq. 2)}$$

Calculation Tool: Simulated using the Ladybug plugin with hourly radiation data for the entire year, followed by cumulative summation and normalization.

2) Heating-Season Solar Radiation per Unit Surface Area (HSU)

Definition: The ratio of total solar radiation received by the building envelope during the heating season (November 15 – March 15 in Xi'an) to its surface area, emphasizing the alignment with winter energy demand.

$$\mathrm{HSU} = \frac{\sum \text{ Heating Season Solar Radiation}}{\sum \text{ Building Surface Area}} \quad \text{(eq. 3)}$$

3)Share of Surface Area above $800kW \cdot h(m^2 \cdot a)^{-1}$ (SA_{800})

Definition: The proportion of building envelope surface area that receives more than the photovoltaic feasibility threshold of $800\ kW \cdot h(m^2 \cdot a)^{-1}$ annual solar radiation.

$$\mathrm{SA}_{800} = \frac{\sum \text{ Surface Area above Threshold}}{\sum \text{ Building Surface Area}} \times 100\% \quad \text{(eq. 4)}$$

Threshold Reference: Proposed by Compagnon (2004) as the economic feasibility threshold for photovoltaic applications.

4)Share of Solar Radiation above $800\ kW \cdot h(m^2 \cdot a)^{-1}$ (SS_{800})

Definition: The proportion of total annual solar radiation incident on the building envelope that exceeds the 800 $kW \cdot h(m^2 \cdot a)^{-1}$ threshold, quantifying the contribution of high-irradiance surfaces and guiding the prioritization of photovoltaic panel placement.

$$\mathrm{SS}_{800} = \frac{\sum \text{ Solar Radiation above Threshold}}{\sum \text{ Solar Radiation}} \times 100\% \quad \text{(eq. 5)}$$

3.Results

3.1. Correlation Between VOF and Solar Potential in Xi' an

The study reveals a significant positive correlation between the Vertical Obstruction Factor (VOF) and solar potential indicators in Xi'an (Table 1). Specifically, VOF shows a Pearson correlation coefficient of 0.580 with the Annual Solar Radiation per Unit Area (ASU), and 0.509 with Heating Season Solar Radiation (HSU), indicating that increased obstruction significantly reduces solar energy acquisition. Furthermore, VOF is positively associated with high-radiation zone indicators, including the Surface Area above $800\ kW \cdot h(m^2 \cdot a)^{-1}$ (SA_{800}) and the Share of Solar Radiation above $800\ kW \cdot h(m^2 \cdot a)^{-1}$ (SS_{800}), confirming its effectiveness in representing the impact of shading on solar availability.

Table 1. Correlation Analysis between Morphological Indicators and Solar Energy Potential of 50 Existing Residential Buildings in Xi'an (Source: Author's Own Work)

Building Morphology Indicator	ASU		HSU		SA_{800}		SS_{800}	
	r	P	r	P	r	P	r	P
VOF	0.580	＜0.01	0.509	＜0.01	0.553	＜0.01	0.563	＜0.01

3.2. Impact of VOF on Solar Potential in Xi'an and Lhasa

The value of VOF is jointly regulated by the building spacing-to-height ratio (D/H) and the gaps between the front-row buildings. Based on the analysis of experimental data in Lhasa, it was found that as the front-row gap increases, the VOF value significantly improves, thereby enhancing the building's solar acquisition potential. However, these studies only considered single-gap variations, while the actual residential layouts are more complex, often involving multiple obstruction sources simultaneously. The VOF indicator can effectively integrate such multi-obstruction effects caused by complex building arrangements, and its variation trend is consistent with that of D/H. Therefore, this study further investigates the mechanisms and thresholds of VOF and solar acquisition potential indicators in Xi'an under different D/H conditions (Tables 2 and 3).

Table 2. Morphological Information of Individual Building Samples with Different D/H Ratios in Xi'an (Source: Author's Own Work)

Sample ID	VOF	Height of Front-Row Obstructing Building H (m)	D/H	Sample ID	VOF	Height of Front-Row Obstructing Building H (m)	D/H
1	0.22	0	0	9	-0.19	24（8F)	1.08
2	0.17	3（1F)	8.67	10	-0.24	27（9F)	0.96
3	0.11	6（2F)	4.33	11	-0.29	30（10F)	0.87
4	0.06	9（3F)	2.89	12	-0.34	33（11F)	0.79
5	0.01	12（4F)	2.17	13	-0.39	36（12F)	0.72
6	-0.04	15（5F)	1.73	14	-0.45	39（13F)	0.67
7	-0.09	18（6F)	1.44	15	-0.50	42（14F)	0.62
8	-0.14	21（7F)	1.24	16	-0.55	45（15F)	0.58

Table 3. Morphological Information of Individual Building Samples with Different D/H Ratios in Lhasa (Source: Author's Own Work)

Sample ID	VOF	Height of Front-Row Obstructing Building H (m)	D/H	Sample ID	VOF	Height of Front-Row Obstructing Building H (m)	D/H
1	0.29	0	0	9	-0.18	24（8F)	1.08
2	0.23	3（1F)	8.67	10	-0.24	27（9F)	0.96
3	0.17	6（2F)	4.33	11	-0.30	30（10F)	0.87
4	0.11	9（3F)	2.89	12	-0.36	33（11F)	0.79
5	0.05	12（4F)	2.17	13	-0.42	36（12F)	0.72
6	-0.01	15（5F)	1.73	14	-0.48	39（13F)	0.67
7	-0.07	18（6F)	1.44	15	-0.54	42（14F)	0.62
8	-0.13	21（7F)	1.24	16	-0.60	45（15F)	0.58

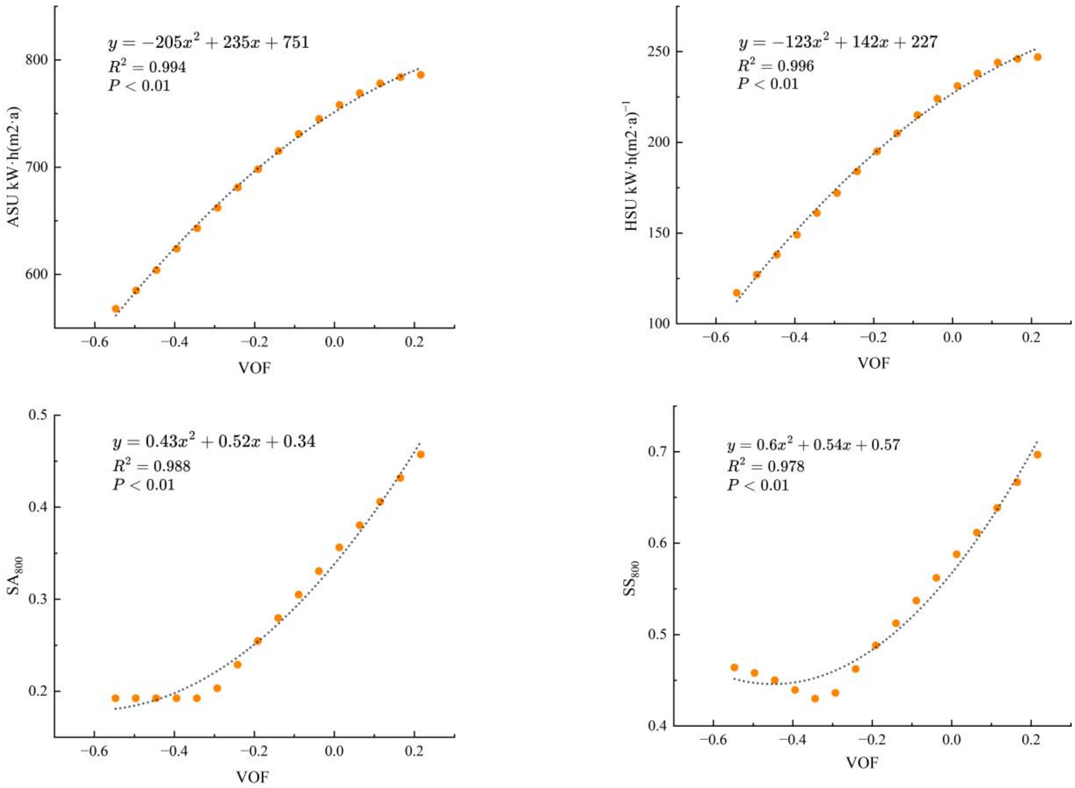

Figure 3. Correlation between Obstruction Factor (VOF) and Solar Energy Potential Indicators in Xi'an

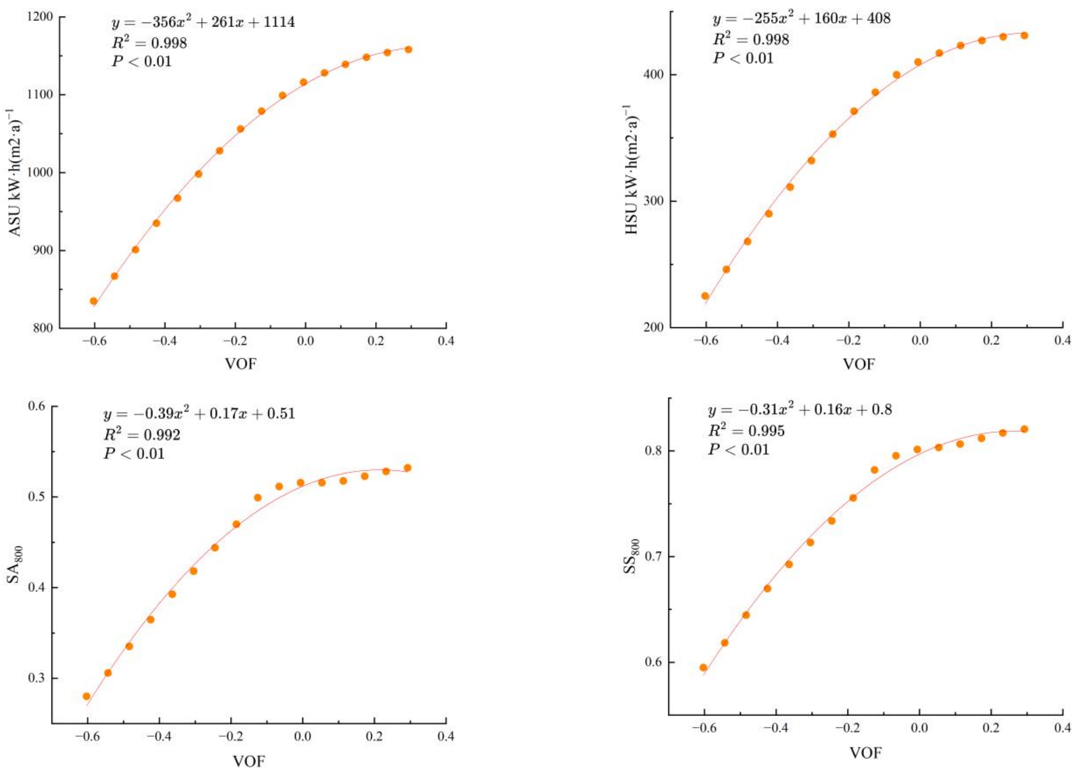

Figure 4. Correlation between Obstruction Factor (VOF) and Solar Energy Potential Indicators in Lhasa

For the same set of typical simulation models, the following results can be observed:

(1) In Xi'an, under the influence of D/H, the VOF shows a near-quadratic relationship with the annual solar radiation per unit external surface area (ASU), heating season solar radiation per unit external surface area (HSU), the percentage of surface area exceeding the threshold (SA_{800}), and the percentage of solar radiation exceeding the threshold (SS_{800}) (Fig. 3) . The fitting coefficients of determination (R^2) are 0.994, 0.996, 0.988, and 0.978, respectively, all of which are statistically significant ($P < 0.01$). As the VOF increases, the degree of obstruction on individual buildings decreases, and all four solar acquisition potential indicators increase accordingly. Both ASU and HSU exhibit a diminishing growth trend, while SA_{800} and SS_{800} remain nearly constant when VOF < －0.4. Specifically, SA_{800} approaches the minimum value of 19% and stabilizes, whereas SS_{800} increases as VOF decreases, because the surface area receiving more than $800 kW \cdot h(m^2 \cdot a)^{-1}$ remains constant, but the total radiation value decreases. When VOF > －0.4, both SA_{800} and SS_{800} increase steadily, with relatively small changes in growth rates.

(2) In Lhasa, under the influence of D/H, the VOF also exhibits a near-quadratic relationship with ASU, HSU, SA_{800}, and SS_{800} (Fig. 4), with R^2 values of 0.998, 0.998, 0.992, and 0.995, respectively, all highly significant ($P < 0.01$). As VOF increases, the degree of obstruction decreases, leading to growth in all four solar acquisition potential indicators. Both ASU and HSU follow a diminishing growth trend, while SA_{800} and SS_{800} approach their maximum values (approximately 51% and 80%, respectively) when VOF > －0.1.

In summary, this regulation ensures to some extent that the solar acquisition potential of buildings is protected from severe inter-building obstruction. However, since building spacing control only guarantees unobstructed solar access from the due-south direction, the actual solar acquisition may still be influenced by southeast or southwest obstructions depending on building layout. Therefore, VOF can serve as a supplementary indicator for assessing inter-building obstruction, providing a more effective means to evaluate the impact of building layout on solar energy acquisition potential.

4.Discussion

Experimental validation in Xi'an demonstrates a significant positive correlation between the Vertical Obstruction Factor (VOF) and solar energy potential indicators. As the building distance-to-height ratio (D/H) increases, the VOF value rises correspondingly, accompanied by simultaneous growth in ASU and HSU, indicating that greater spacing effectively improves solar accessibility. Comparative analysis between Lhasa and Xi'an reveals that in both regions, solar acquisition increases with VOF, yet their response characteristics differ markedly. The growth rate of the response curve gradually decreases in both cities, with Xi'an exhibiting a distinct low-threshold feature, while Lhasa shows a pronounced high-threshold characteristic.

In the typical model analysis, the shaded building in Lhasa is twelve stories high, and as the shading building height increases from 1 to 15 stories, the VOF fluctuates between 0.23 and －0.60, corresponding to a D/H decrease from 8.67 to 0.58. In Xi'an, the shaded building is twelve stories high, and when the shading building height varies from 1 to 15 stories, the VOF ranges from 0.16 to －0.54, with D/H decreasing from 8.67 to 0.58. The results indicate that in high-density urban areas of Xi'an, when VOF > －0.35, the shading effect weakens significantly, marking a critical point for improving solar exposure in dense urban blocks. This demonstrates that VOF, as a comprehensive indicator of inter-building obstruction, effectively captures the relationship between urban morphology and solar energy potential.

Further analysis of the SS_{800} and SA_{800} indices reveals pronounced threshold behaviors, reflecting a nonlinear response between VOF and solar acquisition potential. In Lhasa, when VOF ⩾ －0.1, SS_{800} approaches 80% and SA_{800} about 55%, forming a distinct upper threshold where shading effects become saturated and further spacing yields diminishing solar gains. In Xi'an, when VOF ⩽ －0.35, SS_{800} drops to about 19% and then stabilizes, while SA_{800} decreases to approximately 42.5% and shows an inflection point.As VOF continues to decrease, SA_{800} slightly increases, because the surface area and solar radiation above the threshold remain constant, while the total radiation continues to decline, resulting in a higher percentage of radiation above the threshold. This indicates the presence of a lower threshold.

Table 4. Partial Samples Used for Correlation Validation

Case No.	Test Building	ASU (kW • h(m2 • a)$^{-1}$)	HSU (kW • h(m2 • a)$^{-1}$)	SA_{800} (kW • h(m2 • a)$^{-1}$)	SS_{800} (kW • h(m2 • a)$^{-1}$)	VOF
1	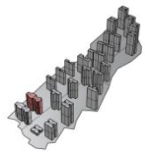	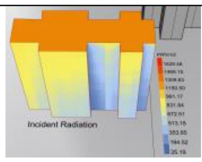 590	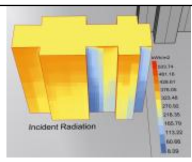 183	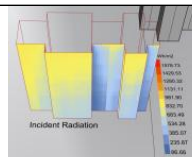 573	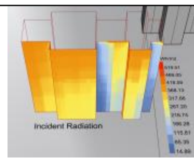 255	-0.66
2	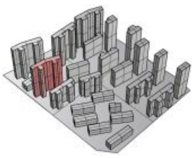	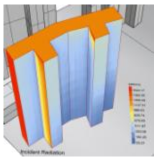 525	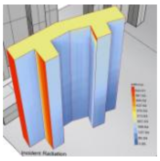 149	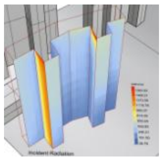 363	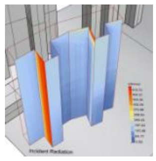 129	-0.48
3	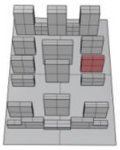	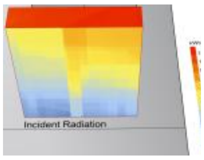 422	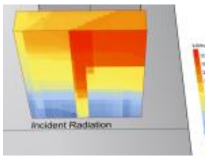 119	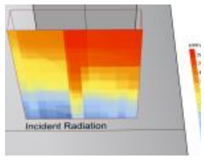 490	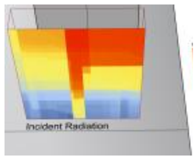 177	-0.56
4	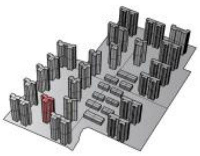	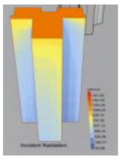 423	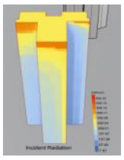 115	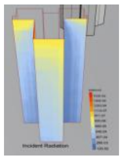 476	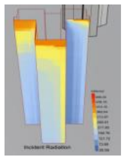 145	-0.61
5	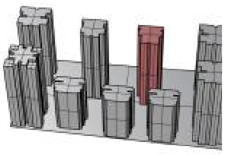	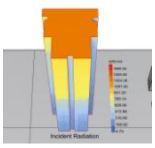 470	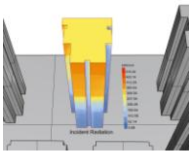 127	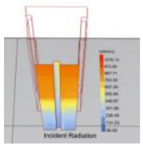 473	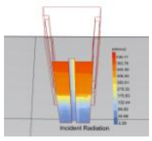 184	-0.66
6		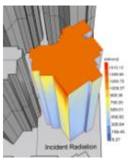 399	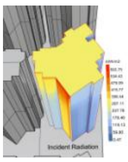 110	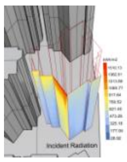 481	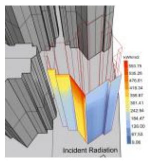 202	-1.48
7	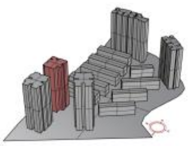	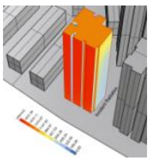 593	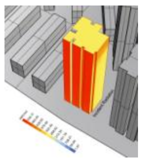 183	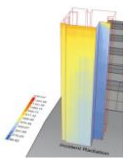 457	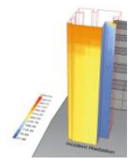 197	-2.09

These threshold differences highlight the regional influence of geographic and climatic factors on building obstruction effects. Lhasa’s higher altitude, greater solar elevation angle, and stronger annual radiation enable near-unshaded conditions under the same geometric settings, whereas Xi'an’s lower solar angles and weaker atmospheric transmissivity lead to stronger shading sensitivity at low VOF values. Thus, the identified thresholds reflect regional boundaries in the solar–morphological response, emphasizing the necessity of climate-specific solar planning strategies. Applying these VOF thresholds as design control parameters can guide spacing and form optimization in solar-responsive urban design, supporting low-carbon and climate-adaptive development.It should be noted that, according to the original definition, a larger VOF value indicates a weaker obstruction condition, corresponding to greater solar radiation received by the building. A VOF value of zero does not represent a completely unobstructed condition but rather serves as a reference point within the calculated range.

Nevertheless, several limitations remain.

(1) The current calculation formula of the Vertical Obstruction Factor (VOF) does not fully capture the morphological characteristics of the obstructed buildings. In the correlation validation, the VOF values of the samples ranged from −0.8 to 0.2. However, the results revealed that when both the obstructed and obstructing buildings were high-rise point blocks with strong mutual shading (such as samples 6 and 7 in Table 4), relatively small VOF values were observed, yet the annual solar radiation per unit area remained high. This contradicts the theoretical logic of the VOF as a quantitative indicator of obstruction, where a smaller VOF value—indicating stronger obstruction—should correspond to a lower annual solar radiation per unit area.

(2) The independent contribution of geographic variables remains indistinguishable. Under the combined influence of solar altitude, annual radiation, and D/H parameters, the statistical model cannot isolate the individual effects of each variable on the VOF–solar relationship.

(3) Although D/H variations were simulated, spacing patterns were primarily linear and regular, excluding multi-row, multi-layer, or irregular configurations commonly found in real urban environments.

(4) The proposed VOF thresholds are derived from a single typical model simulation rather than full regional statistics; therefore, they serve as reference values for comparative analysis rather than universal standards. Future studies should integrate diverse urban typologies and field-measured datasets to refine and validate the applicability of VOF across different climatic regions.

5.Conclusion

This study validated the applicability of the Vertical Obstruction Factor (VOF) in Xi'an and further extended its use as a cross-regional assessment tool for building solar energy potential. Through empirical analysis of 50 residential community samples and comparative studies using typical models, the results indicate that VOF is significantly positively correlated with solar energy potential indicators (ASU, HSU, SA_{800}, and SS_{800}) in Xi'an ($p < 0.01$). VOF effectively reflects the shading trends and radiation responses induced by variations in the building height-to-spacing ratio (D/H).

Cross-regional comparison revealed significant differences in VOF response curves and key thresholds between Xi'an and Lhasa. In high-density residential areas of Xi'an, the minimum VOF threshold is approximately –0.35, exhibiting an approximately linear increase with solar energy potential indicators. In contrast, in Lhasa, the maximum VOF threshold is around –0.1, and its growth trend gradually diminishes. These differences are primarily attributed to geographic conditions, such as variations in solar altitude due to latitude and differences in annual total solar radiation, rather than building layout alone.

Overall, the VOF indicator not only captures the influence of geographic factors on solar energy accessibility but also reveals the regulatory effect of urban morphological features (e.g., building density and layout patterns) on solar radiation distribution. This underscores the importance of fully considering local climate and spatial characteristics when formulating region-specific solar energy utilization strategies.

It should be noted that the critical VOF thresholds proposed in this study are based on simulations of typical models rather than statistical conclusions for the entire region. Their primary role is to quantitatively reveal the relationship between shading effects and radiation response under controlled model conditions, providing a reference for further research. Future studies could combine VOF with in-situ measurements from different cities to validate the applicability of these thresholds, optimize the algorithm for complex building forms and irregular layouts, and integrate VOF into architectural design practice as a spatial optimization tool during the planning stage of residential communities, enabling the assessment of building cluster solar potential.

6.Acknowledgments

The research of this paper was supported by the National Natural Science Foundation of China (No. 52078422).Gratitude is extended to Wenqiang Li for proposing the Vertical Obstruction Factor (VOF), which forms the foundation of this study. Thanks are also given to members of the Sustainable Building and Environmental Research group at the Northwestern Polytechnical University for their valuable discussions and assistance during the research process.

7.References

Compagnon, R. 2004. Solar and daylight availability in the urban fabric. Energy and Buildings, 36**,** 321-328.

Ibrahim, Y., Kershaw, T., Shepherd, P. & Elkady, H. 2022. Multi-objective optimisation of urban courtyard blocks in hot arid zones. Solar Energy, 240**,** 104-120.

Li, J., He, Z. & Zhao, B. 2024. A novel method of high-density urban block form generation based on multi-objective solar performance optimization: A case study of Nanjing. Energy and Buildings, 324**,** 114878.

Li, W. 2023. Research on Residential Morphological Design Control Indicators Based on Solar Energy Acquisition Potential: A Case Study of Lhasa. Master's thesis, Northwestern Polytechnical University.

Liu, B., Liu, Y., Cho, S. & Chow, D. H. C. 2024. Urban morphology indicators and solar radiation acquisition: 2011-2022 review. Renewable & Sustainable Energy Reviews, 199.

Mahaya, C., Zemmouri, N., Benharra, H. & Elnokaly, A. 2022. Solar Access Assessment in Semi-Arid Urban Context: An Application Study for Ten Urban Forms of Existing Apartment Buildings Districts in Batna City, Algeria. Sustainable Cities and Society, 83.

Poon, K. H., Kampf, J. H., Tay, S. E. R., Wong, N. H. & Reindl, T. G. 2020. Parametric study of URBAN morphology on building solar energy potential in Singapore context. Urban Climate, 33.

Tian, J. & Xu, S. 2021. A morphology-based evaluation on block-scale solar potential for residential area in central China. Solar Energy, 221**,** 332-347.

Wenqiang, L., Yu, L., Guorui, S., Wuxing, Z., Jin, W., Teng, S., Yufei, Z., Yiming, Z., Minmin, Y. & Jie, S. 2022. A Calculation Method for Building Solar Energy Acquisition Potential Indicator. 2025-08-15.

Yang, Y., Hsieh, C.-M. & Wu, X.-Y. 2024. How the urban morphology affects the suitable solar energy techniques and performance: A block-scale study based on the typological method in Macau. Solar Energy, 275**,** 112620.

Zhu, D., Song, D., Shi, J., Fang, J. & Zhou, Y. 2020. The Effect of Morphology on Solar Potential of High-Density Residential Area: A Case Study of Shanghai. Energies, 13.